Kinetic Mechanism and Intrinsic Isotope Effects for the Peptidylglycine α-Amidating Enzyme Reaction†

Wilson A. Francisco,‡ David J. Merkler,§ Ninian J. Blackburn,|| and Judith P. Klinman*,‡,⊥

Departments of Chemistry and of Molecular and Cell Biology, University of California, Berkeley, California 94720-1460, Department of Chemistry and Biochemistry, Duquesne University, Pittsburgh, Pennsylvania 15282-1530, and Department of Chemistry, Biochemistry, and Molecular Biology, Oregon Graduate Institute of Science and Technology, P.O. Box 91000, Portland, Oregon 97291-1000

Received December 8, 1997; Revised Manuscript Received April 6, 1998

ABSTRACT: The bifunctional peptidylglycine α-amidating enzyme catalyzes the C-terminal amidation of glycine-extended peptides. The first enzyme activity, peptidylglycine α-hydroxylating monooxygenase, catalyzes the oxygen-, ascorbate-, and copper-dependent formation of α-hydroxyglycine derivatives. These are substrates for the second enzyme activity, peptidylamidoglycolate lyase, which catalyzes their breakdown to the corresponding C-terminal amidated peptide and glyoxylate as final products. Kinetic and isotope effect studies were carried out with *N*-benzoylglycine as a substrate at pH 6.0 using monofunctional and bifunctional monooxygenase activities. Kinetic data indicate an equilibrium ordered mechanism, with hippuric acid binding first followed by oxygen. A potentially important difference between the two monooxygenase activities is that product release occurs more slowly from the bifunctional enzyme, indicating an influence of the lyase domain on release of α-hydroxyglycine product to solution. Intrinsic isotope effects for the C−H bond cleavage were measured for the monofunctional form of the enzyme using a double-label tracer method, yielding 10.6 ± 0.8 and 1.20 ± 0.03 for the primary and α-secondary deuterium intrinsic isotope effects, respectively. These values are identical to previous measurements for the analogous enzyme system, dopamine *β*-monooxygenase [Miller, S. M., and Klinman, J. P. (1985) *Biochemistry 24*, 2114−2127]. The identity of intrinsic isotope effects for peptidylglycine α-hydroxylating monooxygenase and dopamine *β*-monooxygenase with substrates of comparable reactivity (*N*-benzoylglycine and dopamine, respectively) extends similarities between the two enzymes significantly beyond sequence homology and cofactor requirements.

Many neuropeptide hormones require an amidated carboxyl terminus for full biological activity (*1*). These amidated hormones are synthesized by the posttranslational modification of peptide precursors carrying a glycine residue in the C terminus by the action of the bifunctional enzyme peptidylglycine α-amidating monooxygenase (PAM)[1] (EC 1.14.17.3) as shown in Scheme 1 (for recent reviews, see refs *1*−*3*). The first enzyme, peptidylglycine α-hydroxylating monooxygenase (PHM), catalyzes the copper-, ascorbate-, and molecular oxygen-dependent stereospecific α-hydroxylation of glycine extended precursors. These α-hydroxyglycine derivatives are then substrates for the second enzyme, peptidylamidoglycolate lyase (PAL) (EC 4.3.2.15), which catalyzes the breakdown of the α-hydroxyglycine derivative to produce the corresponding C-terminal amidated peptide and glyoxylate as the final products.

The reaction catalyzed by peptidylglycine α-amidating monooxygenase is similar to the reaction catalyzed by dopamine *β*-monooxygenase (D*β*M). This latter enzyme catalyzes the conversion of dopamine to norepinephrine in a copper-, ascorbate-, and molecular oxygen-dependent reaction. The amino acid sequences of PHM and D*β*M are 32% identical (*4*, *5*). Both enzymes bind two coppers atoms (*6*−*8*) and cycle through Cu(II) and Cu(I) redox states during catalysis (*9*−*12*). The crystal structure for the catalytic core of PHM has recently been solved, showing that the copper centers are at a distance of 11 Å residing on separate domains that are solvent-exposed (*13*).

The kinetic mechanism of PAM has yet to be fully characterized. Previous kinetic experiments have focused upon the relative order of binding of ascorbate and peptide substrate and the stoichiometry and products of the reaction between ascorbate and enzyme (*14*−*16*). These experiments have shown that ascorbate binds first, reducing Cu(II) to Cu(I) with the release of semidehydroascorbate, before peptide and dioxygen bind (*17*). This is in agreement with the kinetic mechanism of D*β*M (*10*, *18*, *19*), although D*β*M has also

† Supported by National Institutes of Health Grants GM 25765 to J.P.K. and R01 NS 27583 to N.J.B. and grants from the Hunkele Foundation, Unigene Laboratories, Inc., and the Duquesne University Faculty Development Fund to D.J.M. W.A.F. was supported by a postdoctoral fellowship from the NIH (F32 GM 17026) and the Ford Foundation.

* To whom correspondence should be addressed.
‡ Department of Chemistry, University of California.
§ Duquesne University.
|| Oregon Graduate Institute of Science and Technology.
⊥ Department of Molecular and Cell Biology, University of California.

[1] Abbreviations: PAM, peptidylglycine α-amidating monooxygenase; PHM, peptidylglycine α-hydroxylating monooxygenase; PAL, peptidylamidoglycolate lyase; D*β*M, dopamine *β*-monooxygenase; PHMcc, catalytic core of PHM; HA, hippuric acid.

S0006-2960(97)03004-3 CCC: $15.00
Published on Web 05/14/1998

Scheme 1

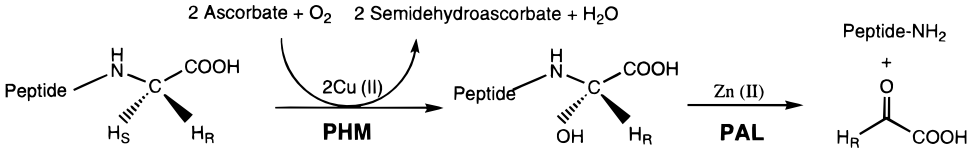

been shown to support copper reduction in the enzyme product complex under conditions of high ascorbate (*10*). There are no kinetic data available concerning the relative order of binding of molecular oxygen and peptide to either PAM or PHM.

Isotope effect measurements provide a valuable tool in the determination of the kinetic mechanism of enzymes. The order of addition of reactants can be obtained from the magnitude of the isotope effects on the kinetic parameters for the various substrates (*20*, *21*). To date, there has been only one report of an isotope effect on the PAM reaction. Kizer et al. (*14*) reported a primary deuterium isotope effect on V_{max} of approximately 6 for the substrate pyro-Glu-His-Pro-Gly.

Hippuric acid (*N*-benzoylglycine) has been shown to be the smallest amide substrate for PAM (*22*). Although this peptide analogue has a K_m value higher than those of the larger peptide substrates, the ease of synthesis of isotopically labeled variants made it an ideal candidate for a complete kinetic study. We now report an extensive kinetic and isotope effect study of the monofunctional and bifunctional forms of the peptidylglycine α-amidating monooxygenase using hippuric acid as a substrate. Labeled hippuric acids were synthesized, and isotope effects were measured on initial rates as a function of substrate and oxygen concentration. Deuterium and tritium isotope effects were also measured competitively to determine the intrinsic isotope effect for the C−H bond cleavage. The relationship of these findings to the analogous copper enzyme dopamine β-monooxygenase is discussed. Although the kinetic mechanism of PAM differs somewhat from that of DβM, the structure of the activated complexes for these enzymes appears to be identical when substrates of similar catalytic efficiency are compared.

MATERIALS AND METHODS

Materials. [2-$^2H_2$]Glycine (98% ^2H) was purchased from Cambridge Isotope Laboratories, Inc. (Andover, MA). [*ring*-U-^{14}C]Benzoic acid (55 mCi/mmol) and sodium [^{3}H]borohydride (100 mCi/mmol) were from American Radiolabeled Chemicals, Inc. (St. Louis, MO). Tritiated water (TOH, 90 mCi/mmol) and Ecolite(+) liquid scintillation cocktail were purchased from ICN Pharmaceuticals, Inc. (Costa Mesa, CA). Glutamate-pyruvate transaminase and catalase were from Boeringer Mannheim Corp. (Indianapolis, IN). Dowex 50WX8-400 ion-exchange resin and 1,3-dicyclohexylcarbodiimide were from Aldrich Chemical Co. (St. Louis, MO). MES and sodium ascorbate were from Sigma (St. Louis, MO). Glycine benzyl ester *p*-toluenesulfonate was from Fluka Chemical Corp. (Ronkonkoma, NY). All other reagents from commercial sources were of the highest purity available and were used without further purification.

*Synthesis of N-[benzoyl-2-$^2H_2$]Glycine (**1**).* The synthesis was performed according to a modification of the procedure of Chen and Benoiton (*23*). To a vigorously stirred solution of [2-$^2H_2$]glycine (0.77 g, 10 mmol) and NaOH (0.40 g, 10 mmol) in 30 mL of water at 0 °C were added benzoyl chloride (1.28 mL, 11 mmol) and diisopropylethylamine (1.98 mL, 11 mmol) alternately in small portions over the course of 30 min. The mixture was stirred for an additional 30 min, then cooled again, and acidified with 6 N HCl until a white solid precipitated. The crude *N*-benzoyl[2-$^2H_2$]-glycine was collected by filtration, triturated in boiling CCl_4 (30 mL), and collected again by filtration. The product was further purified by recrystallization from H_2O: yield 1.26 g (70%); mp 186−189 °C (lit. mp 186−187 °C); MS (EI^+) *m*/*z* (relative intensity) 181 (43), 137 (47), 105 (100), 77 (67).

*Synthesis of N-[ring-U-^{14}C]Benzoylglycine (**2**).* *N*-[*ring*-U-^{14}C]Benzoylglycine benzyl ester was synthesized by adding triethylamine (13 μL, 0.092 mmol) and 1,3-dicyclohexylcarbodiimide (19 mg, 0.092 mmol) to a mixture of glycine benzyl ester *p*-toluenesulfonate (31 mg, 0.092 mmol) and [*ring*-U-^{14}C]benzoic acid (1 mCi, 10 mCi/mmol) in CH_2Cl_2 (1 mL). The reaction mixture was stirred at 0 °C for 1 h and at room temperature for 18 h and filtered and the precipitate washed with CH_2Cl_2 (2 mL). The filtrate was washed with H_2O (2 × 1 mL), dried (Na_2SO_4), filtered, and evaporated. The benzyl protecting group was removed by a modification of the procedure of Anantharamaiah and Sivanandaiah (*24*). To the crude *N*-[*ring*-U-^{14}C]benzoylglycine benzyl ester was added a mixture of ethanol (5 mL), cyclohexene (2.5 mL), and 10% palladium on charcoal (10 mg), and the mixture was refluxed with stirring for 3 h. The catalyst was removed by filtration and washed with hot ethanol (5 mL). The solvent was removed in vacuo to yield the crude product which was purified by semipreparative reversed-phase HPLC on a Dynamax 300 Å C18 column (Rainin) with an isocratic system of 2% CH_3CN in 50 mM ammonium acetate (pH 5.5). The collected fractions were pooled, lyophilized, redissolved in 1% ethanol, and stored frozen. The final specific activity of the product was 9.5 μCi/mmol.

*Synthesis of N-[ring-^{3}H]Benzoyl-(2S)-[2-$^2H_1$]glycine (**3**).* (2*S*)-[2-$^2H_1$]Glycine was prepared by a modification of the method of Gani et al. (*25*). To a solution of [2-$^2H_2$]glycine (100 mg, 1.30 mmol) in 2 mL of 100 mM potassium phosphate (pH 7.6) was added glutamate-pyruvate transaminase (100 units), and the reaction mixture was incubated at 37 °C in the dark. No pyridoxal 5′-phosphate was added to the mixture as suggested by Gani et al. (*25*) to avoid any nonenzymatic hydrogen exchange. After 24 and 48 h, another portion of glutamate-pyruvate transaminase (100 units) was added to the mixture. The solution was incubated for a total of 96 h, after which the enzyme was denatured by boiling for several minutes. The mixture was centrifuged and the supernatant solution frozen and lyophilized to yield (2*S*)-[2-$^2H_1$]glycine and buffer. (2*S*)-[2-$^2H_1$]Glycine was purified by ion-exchange chromatography by dissolving the

reaction mixture in 0.1 N HCl and loading it onto a Dowex 50WX8-400 column (H^+ form, 1 × 10 cm). The column was washed with H_2O (100 mL), and the glycine was eluted with 3 M NH_4OH (50 mL). The ninhydrin-positive fractions were pooled and lyophilized. The glycine was characterized as its camphanic acid (*25*). For the *N*-camphanoyl-(2*R*)-[2-$^2H_1$]glycine derivative, stereochemical purity of >99% and deuterium content of >99 at. % was found by NMR and mass spectrometry analysis, respectively. [*ring*-^{3}H]Benzoic acid was synthesized by the rhodium(III) chloride-catalyzed exchange procedure for the TOH titration of aromatic carboxylic acids (*26*). [*ring*-^{3}H]Benzoyl chloride was prepared from [*ring*-^{3}H]benzoic acid using cyanuric chloride (*27*). [*ring*-^{3}H]Benzoic acid (18 mg, 0.15 mmol) and cyanuric chloride (13.8 mg, 0.075 mmol) were dissolved in acetone (1 mL), and the mixture was stirred at room temperature. Triethylamine (21 μL, 0.15 mmol) was added, and a white precipitate formed immediately. The reaction mixture was stirred for 2 h, the acetone removed in vacuo, and the precipitate extracted with CCl_4 (4 × 1 mL). The combined CCl_4 fractions were filtered, and the CCl_4 was removed in vacuo to yield [^{3}H]benzoyl chloride. The [^{3}H]-benzoyl chloride was placed in an ice bath, and a solution of (2*S*)-[2-$^2H_1$]glycine (11.3 mg, 0.15 mmol) in 0.5 M NaOH (600 μL, 0.30 mmol) was added and the mixture stirred at 0 °C for 15 min and at room temperature for 1 h. The reaction mixture was cooled in an ice bath and acidified with 1 N HCl. The crude *N*-[*ring*-^{3}H]benzoyl-(2*S*)-[2-$^2H_1$]glycine was purified by semipreparative reversed-phase HPLC on a Dynamax 300 Å C18 column with an isocratic system of 2% CH_3CN in 50 mM ammonium acetate (pH 5.5). The collected fractions were pooled, lyophilized, redissolved in 1% ethanol, and stored frozen. The final specific activity of the product was 11.7 μCi/mmol.

*Synthesis of N-Benzoyl-(RS)-[2-^{3}H]glycine (**4**).* (*RS*)-[2-^{3}H]Glycine was synthesized by sodium [^{3}H]borohydride reductive amidation of glyoxylate as described by Denu and Fitzpatrick (*28*). To a vigorously stirred solution of (*RS*)-[2-^{3}H]glycine (15 mg, 0.2 mmol) in 0.8% NaOH (2.25 mL, 0.45 mmol) at 0 °C was added benzoyl chloride (35 μL, 0.30 mmol), and the reaction mixture was stirred at 0 °C for 15 min and at room temperature for 1 h. The reaction mixture was cooled to 0 °C and acidified with 1 N HCl. The crude *N*-[*ring*-^{3}H]benzoyl-(*RS*)-[2-^{3}H]glycine was purified by semipreparative reversed-phase HPLC on a Dynamax 300 Å C18 column with an isocratic system of 2% CH_3CN in 50 mM ammonium acetate (pH 5.5). The collected fractions were pooled, lyophilized, redissolved in 1% ethanol, and stored frozen. The final specific activity of the product was 2.8 μCi/mmol.

Enzyme Preparation. Chinese hamster ovary cells which secrete recombinant type A rat medullary carcinoma PAM into the culture medium were grown in a Wheaton stirred tank bioreactor (*29*). The bifunctional 75 kDa enzyme was purified as described by Miller et al. (*30*). Catalytic core PHM (PHMcc) was purified as described by Kolhekar et al. (*31*).

Noncompetitive Kinetic Isotope Effects. Initial velocities were measured at varied oxygen and *N*-benzoylglycine or *N*-benzoyl[2-$^2H_2$]glycine concentrations by the rate of oxygen consumption at 37 °C and pH 6.0. The decrease in oxygen concentration was measured with a YSI model 5300 biological oxygen monitor. The temperature of the chamber was maintained at 37 ± 0.1 °C with a Neslab circulating water bath. Reaction mixtures (1 mL) contained 100 mM MES (pH 6.0), 30 mM KCl, 10 mM sodium ascorbate, 10 mg/mL catalase, 1 μM $CuSO_4$, and various amounts of *N*-benzoylglycine or *N*-benzoyl[2-$^2H_2$]glycine (0.1−20 mM). Individual reaction mixtures were made from stock solutions with addition of concentrated solutions of ascorbate, catalase, and $CuSO_4$. Oxygen concentrations were varied by stirring reaction mixtures for at least 15 min with premixed O_2/N_2 mixtures in the appropriate proportions to yield the desired O_2 concentration. The resulting oxygen concentration was determined from the known concentration of dissolved oxygen under conditions of air-saturated water (217 μM at 37 °C). Stock solutions of *N*-benzoylglycine substrates were obtained by weighing samples and dissolving these up to known volumes of 100 mM MES (pH 6.0) and 30 mM KCl buffer. Reactions were initiated by the addition of enzyme (2−5 μL). Velocities for both unlabeled and dideuterated substrates at a given oxygen concentration were obtained in a single experiment using the same stocks of the other reaction components to minimize fluctuations in experimental conditions.

Data from the initial velocity experiments were fit directly to eq 1 using the program Kaleidagraph. The $^D(V/K_{app})$ and $^DV_{app}$ values at a given *N*-benzoylglycine or oxygen concentration were calculated by direct comparison of the *V*/*K* and *V* values for the protiated and dideuterated substrates.

$$v = \frac{VS}{K + S} \tag{1}$$

Data obtained by varying the concentration levels of the two substrates were fitted to eqs 2 or 3 using the programs of Cleland (*32*).

$$v = \frac{VAB}{K_{ia}K_b + K_bA + K_aB + AB} \tag{2}$$

$$v = \frac{VAB}{K_{ia}K_b + K_bA + AB} \tag{3}$$

where *A* and *B* are the substrate concentrations, *V* is the maximal velocity, K_a and K_b are the Michaelis constants for A and B, respectively, and K_{ia} is the dissociation constant of A.

Competitive Kinetic Isotope Effects. These experiments were performed in 100 mM MES (pH 6.0), 30 mM KCl, 10 mM sodium ascorbate, 15 mM potassium iodide, and 100 mg/mL catalase under an atmosphere of oxygen. All reaction mixtures were stirred with the aid of a stir bar and an air-driven magnetic stirrer. The temperature was kept at 37 ± 0.1 °C with a Neslab water bath. The final concentration of hippuric acid was 10 mM, with a ^{3}H:^{14}C ratio of approximately 10. In each experiment, three 50 μL samples at $t = 0$ and six to eight 50 μL samples at various reaction times were removed and the reactions quenched with 1 M $HClO_4$ (10 μL). Samples were then frozen and stored at −70 °C until they were analyzed by HPLC. The samples were thawed, centrifuged for 5 min immediately before HPLC analysis, and injected into a Beckman's Ultrasphere C18-IP column (4.5 mm × 250 mm) equilibrated with 1% CH_3CN in 50 mM ammonium acetate (pH 5.5). After

Table 1: Kinetic Parameters for PAM and PHM[a]

	PAM			PHM		
parameter	[$^1H_2$]HA	[$^2H_2$]HA	IE[b]	[$^1H_2$]HA	[$^2H_2$]HA	IE
V_{max} (s^{-1})	36.8 ± 0.09	36.6 ± 2.8	1.00 ± 0.08	39.1 ± 0.5	25.0 ± 1.1	1.56 ± 0.07
V/K_{O_2} (mM^{-1} s^{-1})	136.8 ± 8.0	44.3 ± 3.1	3.08 ± 0.28	185.0 ± 0.6	58.3 ± 3.9	3.17 ± 0.21
K_i(HA) (mM)	5.0 ± 0.4	8.5 ± 0.8	0.59 ± 0.07	2.9 ± 0.1	4.5 ± 0.4	0.64 ± 0.06

[a] Kinetic parameters obtained by fitting the initial velocity data to the equation describing an equilibrium ordered mechanism (eq 3) using the programs of Cleland (*32*). Experimental conditions were as follows: 100 mM MES (pH 6.0), 30 mM KCl, 10 mg/mL catalase, 1 μM $CuSO_4$, 10 mM ascorbic acid, and varying amounts of protiated and dideuterated hippuric acid and oxygen at 37 °C. [b] IE, isotope effect.

injection of the sample, the same eluent was used for 25 min, followed by a 10 min 1 to 20% acetonitrile gradient and a 5 min 20% acetonitrile. Tritiated water eluted at the dead volume (2.6 min), followed by α-hydroxyhippuric acid (12 min), hippuric acid (23 min), and benzamide (38 min). No benzamide was detected in experiments with PHM. The lack of benzamide formation using PHM is consistent with model studies of carboxamide dealkylation at pH 6.0 (*33*, *34*). Fractions (1.5 mL) were collected and mixed with Ecolite(+) liquid scintillation cocktail (12 mL) and measured in a LKB Wallac model 1209 Rackbeta liquid scintillation counter (5 min/sample). Isotope effects were calculated according to eq 4

$$\frac{k_H}{k_L} = \frac{\ln(1-f)}{\ln\left(1 - f\frac{R_p}{R_\infty}\right)} \quad (4)$$

where L represents D or T, f is the fractional conversion of substrates to products, and R_p and R_∞ are ^3H:^{14}C ratios in products at fractional conversions and 100% conversion, respectively. The fractional conversion was determined from the ratio of ^{14}C in product to the total ^{14}C in product and substrate. Since R_0 routinely equaled R_∞ for the deuterium isotope effect experiment and $R_0/2$ equaled R_∞ for the tritium isotope effect experiments, the average of three R_0 values (or $R_0/2$ for k_H/k_T) was used as R_∞ in eq 4.

RESULTS

Steady-State Kinetics and Isotope Effects. To determine the kinetic mechanism of PAM and PHM, initial velocities were measured as a function of oxygen and protiated and dideuterated hippuric acid. The initial rate patterns obtained for both PAM and PHM (data not shown) are characteristic of an equilibrium ordered mechanism (*35*). The lines on the $1/[O_2]$ versus $1/v$ plot intersect on the $1/v$ axis, indicating a value of 0 for K/V for hippuric acid. The 1/[HA] plot intersects to the left of the $1/v$ axis above the horizontal axis with a $1/v$ coordinate equal to $1/V_{max}$ (data not shown). Secondary plots for both enzymes are also indicative of an equilibrium ordered mechanism. The plot of the slope of 1/[HA] versus $1/[O_2]$ is linear with an intercept at the origin (data not shown).

The initial velocity data as a function of protiated and dideuterated hippuric acid and oxygen obtained for both PAM and PHM were fitted to eqs 2 and 3 describing a steady-state ordered and an equilibrium ordered mechanism, respectively (*32*). The K_a values obtained when fitting the initial velocity data to eq 2 are either extremely small or negative with standard errors larger than the corresponding values, indicating a lack of significance for this term. The

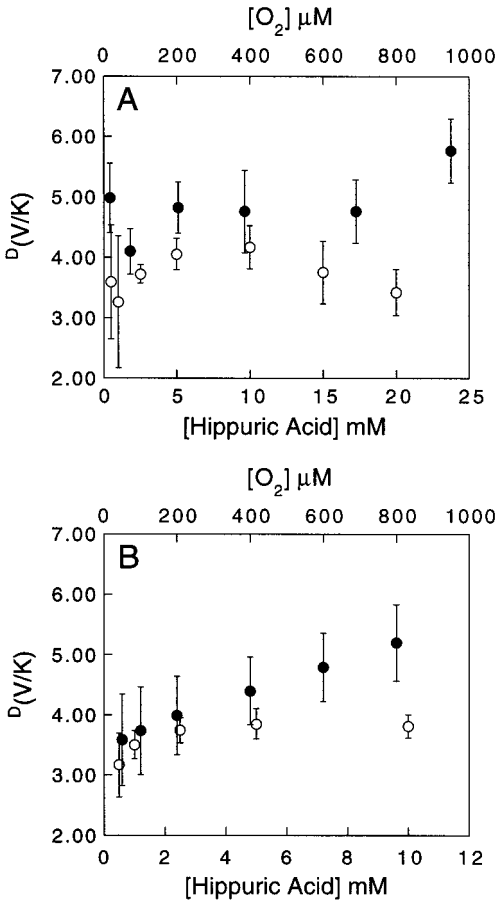

FIGURE 1: Dependence of $^D(V/K)_{HA}$ (●) and $^D(V/K)_{O_2}$ (○) on the concentrations of oxygen and hippuric acid, respectively, for PAM (A) and PHM (B).

kinetic parameters obtained from the fit to eq 3 of the PAM and PHM data are summarized in Table 1.

The isotope effects on $^D(V/K)$ for either substrate as a function of the other for PAM and PHM are shown in Figure 1. $^D(V/K)$ values for both substrates are approximately equal and remain relatively constant as a function of the concentration of the alternate substrate.

Intrinsic Isotope Effects. Northrop (*36*) has provided an elegant method for the determination of the intrinsic isotope effect from the measured deuterium and tritium isotope effects on V/K under identical conditions. In cases where the reverse commitment to catalysis is near zero (i.e., irreversible reactions), it is possible to calculate a unique solution to the intrinsic isotope effect, ^Dk, as described in eq 5.

$$\frac{^D(V/K) - 1}{^T(V/K) - 1} = \frac{^Dk - 1}{^Dk^{1.442} - 1} \quad (5)$$

Scheme 2

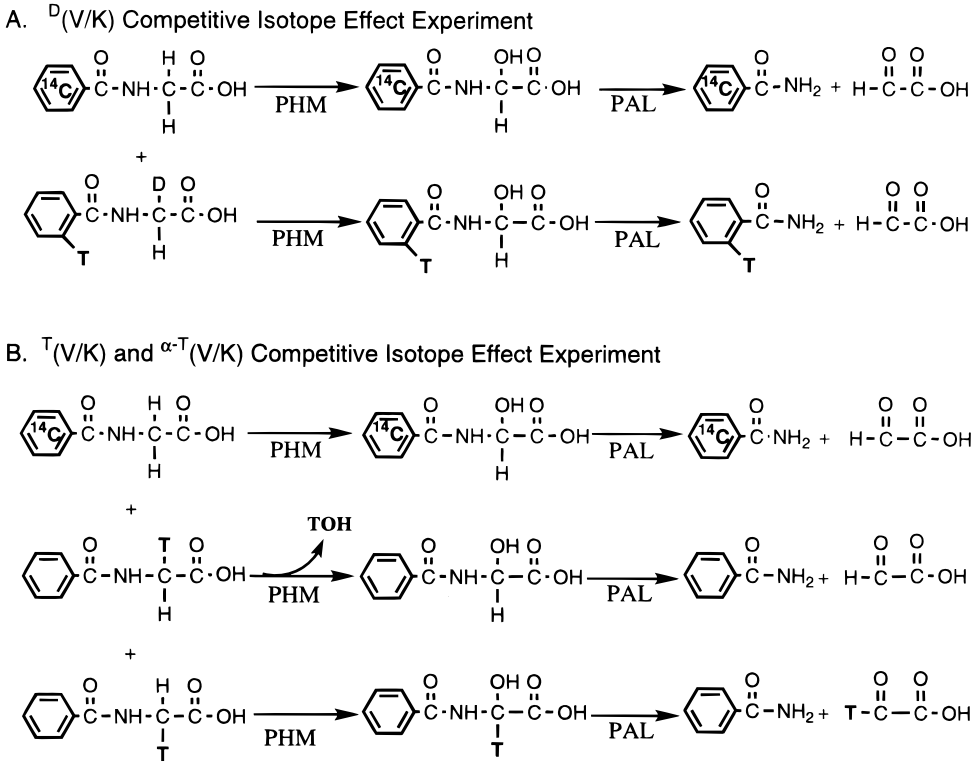

This transcendental equation suffers from the disadvantage that the errors in the measured parameters are inflated in the propagation of errors. For this reason, it is important to measure the deuterium and tritium isotope effects with high precision. To accomplish this, a double-isotope technique was used, as has been done previously with dopamine β-monooxygenase (*37*), among other systems.

Hippuric acid was found to be an excellent candidate for the determination of the intrinsic isotope effect for the C−H bond cleavage since it shows a measurable $^{D}(V/K)_{HA}$. Doubly labeled hippuric acid substrates were synthesized as described in Materials and Methods and used for the measurement of the deuterium and tritium isotope effects. While in the noncompetitive isotope effect measurements dideuterated hippuric acid was used due to the availability of the precursor dideuterated glycine, for the competitive isotope effect measurements, stereospecifically deuterated hippuric acid was synthesized and used. Stereospecifically labeled substrate offers the advantage that the measured isotope effect is a function of the primary intrinsic isotope effect and not of the product of the intrinsic primary and intrinsic α-secondary isotope effects. The use of a randomly labeled tritiated substrate provided the additional advantage that the primary and secondary tritium isotope effects could be measured in a single experiment. The labeled substrates and the corresponding products are shown in Scheme 2. The measured primary deuterium [$^{D}(V/K)$] and primary [$^{T}(V/K)$] and secondary tritium [$^{\alpha-T}(V/K)$] isotope effects for PHM are shown in Figure 2 as a function of fractional conversion and summarized in Table 2. It can be clearly observed that the measured isotope effects are independent of the fractional conversion and that this method allowed for the very precise measurement of isotope effects, with relative errors of <3%.

The isotope effects for PAM were also measured in the same way. The tritiated products with the bifunctional enzyme in the tritium isotope effect experiment are TOH, glyoxylate, and α-hydroxyhippuric acid (Scheme 2). To separate glyoxylate from TOH and α-hydroxyhippuric acid, derivatization of glyoxylate with phenylhydrazine was required. Consistently, we were unable to obtain a quantita-

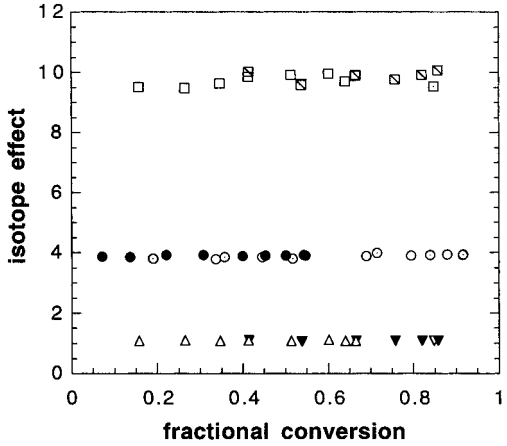

FIGURE 2: $^{D}(V/K)$ (circles), $^{T}(V/K)$ (squares), and $^{\alpha-T}(V/K)$ (triangles) vs fractional conversion for the reaction of hippuric acid with PHM. Independent experiments are represented by different symbols. Experimental conditions are described in Materials and Methods.

Table 2: Competitive Isotope Effects[a]

parameter	PAM	PHM
$^{D}(V/K)_{HA}$	3.82 ± 0.06	3.88 ± 0.05
$^{T}(V/K)_{HA}$	nd[b]	9.73 ± 0.19
$^{\alpha-T}(V/K)_{HA}$	nd	1.09 ± 0.01

[a] Experimental conditions were as follows: 100 mM MES (pH 6.0), 30 mM KCl, 10 mM sodium ascorbate, 15 mM KI, 100 mg/mL catalase, and 1 μM $CuSO_4$ under an atmosphere of oxygen at 37 °C. [b] nd, not determined.

Table 3: Comparison of Intrinsic Parameters for DβM and PHM with Dopamine and Hippuric Acid as Substrates

parameter	DβM	PHM[a]
$^{D}k_5$	10.9 ± 1.9[b]	10.6 ± 0.8
$^{\alpha-D}k_5$	1.19 ± 0.06[c]	1.20 ± 0.03
k_5 (s^{-1})	1200 ± 540[d]	810 ± 120
BDE[e] (kcal/mol)	85[f]	87[g]

[a] Experimental conditions were as follows: 100 mM MES (pH 6.0), 30 mM KCl, 10 mM sodium ascorbate, 15 mM KI, 100 mg/mL catalase, and 1 μM $CuSO_4$ under an atmosphere of oxygen at 37 °C. [b] Taken from ref *37*. [c] Taken from ref *39*. [d] Taken from ref *47*. [e] BDE, bond dissociation energy. [f] Taken from ref *48*. [g] Taken from ref *49*.

tive recovery of the tritiated glyoxylate as the glyoxylate phenylhydrazone, either due to incomplete derivatization or due to degradation of the glyoxylate product before derivatization. For this reason, the tritium isotope effects measured with the bifunctional form of the enzyme were not reproducible. The deuterium isotope measurements did not suffer from this problem since the only labeled products were α-hydroxyglycine and benzamide (Scheme 2) and no derivatization was needed for the HPLC separation. The results of the deuterium isotope effects for PAM are also shown in Table 2. It is clear that the $^{D}(V/K)_{HA}$ values measured with PAM and PHM are identical.

With the results of the deuterium and tritium isotope effect experiments, it is possible to calculate the intrinsic primary isotope effect for the C−H bond cleavage using eq 5. An intrinsic primary deuterium isotope effect (^{D}k) of 10.6 ± 0.8 was obtained. The standard error for the intrinsic isotope effect was calculated as previously described (*38*). With the intrinsic isotope effect and the measured secondary tritium isotope effect, it is possible to calculate the secondary intrinsic isotope effect (*39*). The α-secondary deuterium intrinsic isotope effect ($^{\alpha-D}k$) was calculated to be 1.20 ± 0.03. These results are summarized in Table 3. We note that both the primary and secondary intrinsic isotope effects calculated for PHM are identical to those calculated for the DβM reaction (*37*, *39*) (Table 3). The implications of this result are discussed below.

DISCUSSION

Kinetic Order. In earlier studies of peptidylglycine α-amidating enzyme, it was shown that the reaction of ascorbate with the enzyme displays ping-pong kinetics (*14*−*16*), with the one-electron oxidation of two molecules of ascorbate reducing the two enzyme-bound copper atoms to produce two molecules of semidehydroascorbate before peptide binds (*17*). In this study, we have determined the relative order of oxygen binding to the Cu(I) form of the enzyme. *N*-Benzoylglycine (hippuric acid) has previously been shown to be the smallest peptide analogue substrate for the enzyme (*22*). This small molecule offers the advantage of being easily synthesized, and labeled substrates were readily accessible (Scheme 2). Furthermore, initial deuterium isotope effect measurements with hippuric acid showed moderate isotope effects on the kinetic parameters. These qualities made this small peptide analogue a perfect candidate for detailed kinetic and isotope effects studies. We have carried out extensive initial velocity and isotope effect measurements as a function of hippuric acid and oxygen concentration with the monofunctional and bifunctional forms of peptidyl amidating enzyme to determine the kinetic mechanism and the intrinsic isotope effect for the C−H bond cleavage.

Scheme 3

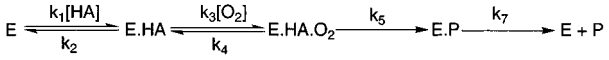

The conventional method for determining an enzyme kinetic mechanism makes use of initial velocity studies in the absence and presence of product and dead-end inhibitors. The reaction catalyzed by PAM and PHM is irreversible, precluding the use of product inhibition and other techniques such as isotopic exchange, commonly used for this purpose. Fortunately, isotope effects have been shown to be a powerful tool for the determination of kinetic mechanisms (*20*, *21*).

Initial velocity patterns obtained with PAM and PHM are indicative of an equilibrium ordered mechanism (Scheme 3 with $k_2 > k_5$). For this mechanism, the addition of the first substrate A (in this case, hippuric acid) is at equilibrium and the intercepts of the 1/[B] reciprocal plot (in this case, O_2) are not affected by changes in the concentration of A (*35*). In other words, double-reciprocal plots intersect on the ordinate when [B] is varied, with the slope replot passing through the origin. The initial velocity data for both PAM and PHM were fitted to the equation describing an equilibrium ordered mechanism (eq 3) (Table 3), and a good fit to this equation was found.

For the kinetic mechanism shown in Scheme 3, the expressions for the isotope effect on V/K for each substrate are shown below:

$$^{D}(V/K)_{HA} = \frac{^{D}k_5 + \dfrac{k_5}{k_2k_4/(k_2 + k_3[O_2])}}{1 + \dfrac{k_5}{k_2k_4/(k_2 + k_3[O_2])}} \quad (6)$$

$$^{D}(V/K)_{O_2} = \frac{^{D}k_5 + \dfrac{k_5}{k_4}}{1 + \dfrac{k_5}{k_4}} \quad (7)$$

For an equilibrium ordered mechanism, k_2 is very fast with respect to $k_3[O_2]$ at any finite level of O_2. Under these conditions, the expression of $^{D}(V/K)_{HA}$ can be reduced to

$$^{D}(V/K)_{HA} = \frac{^{D}k_5 + \dfrac{k_5}{k_4}}{1 + \dfrac{k_5}{k_4}} \quad (8)$$

Therefore, the isotope effect for an equilibrium ordered mechanism will be constant, with $^{D}(V/K)_{HA}$ equal to $^{D}(V/K)_{O_2}$ independent of the concentration of the alternate substrate that is varied. The concentration dependence of the isotope effects on V/K for PAM and PHM (Figure 1) is consistent with such a mechanism.

An equilibrium ordered mechanism is not unreasonable for such a small peptide analogue. The natural substrates for peptidylglycine α-amidating enzyme are large peptides,

and binding interactions between the enzyme and the peptide substrate may be expected to extend beyond the terminal glycine residue. Tamburini et al. (*40*) have shown that the peptide structural elements for peptidylglycine α-amidating enzyme substrate recognition are located within the terminal pentapeptide segment. Furthermore, although the V_{max} for hippuric acid is comparable to those of larger peptide substrates, the V/K_{HA} is approximately 100−500-fold smaller than those measured for the larger peptides (i.e., the K_m for hippuric acid is increased about 100−500-fold) (*41*, *42*). Thus, in the case of extended peptide substrates, the k_2 rate (Scheme 3) may be slowed sufficiently to convert the kinetic mechanism from one that is equilibrium ordered to steady-state ordered.

One discrepancy with the equilibrium ordered mechanism is that fitting the kinetic data to eq 3 (Table 1) leads to an inverse isotope effect on K_{ia} for hippuric acid [$[K_{ia}([^1H_2]HA)]/[K_{ia}([^2H_2]HA)]$ is 0.59 ± 0.07 for PAM and 0.64 ± 0.06 for PHM]. An isotope effect of this magnitude for the dissociation of hippuric acid to peptidyl α-amidating enzyme is unexpected. It is commonly assumed that the binding of isotopically labeled molecules to enzyme active sites is either unaffected or little affected by the isotopic label. Although there have been reports of isotope effects on binding of substrates to enzymes, the isotope effects are small. For example, LaReau et al. (*43*) reported an isotope effect of 1.1 for the binding of isotopically labeled NAD^+ to lactate dehydrogenase. For a mechanism in which substrate binding is in rapid equilibrium, the binding interactions between the substrate and the enzyme are expected to be weak and would be difficult to reconcile with a large isotope effect on binding. The reason for the unexpected isotope effect on K_{ia} is not known at this time and will require further analysis.

The ordered mechanism presented in Scheme 3 indicates that the two substrates combine with the enzyme in an obligate order: O_2 can bind only to the E·HA complex. This could be, for example, the result of a conformational change in the enzyme induced by the binding of the peptidic substrate. Carbon monoxide has commonly been used as a probe of dioxygen binding to Fe(II) and Cu(I) centers in proteins because it has an electronic structure and a mode of binding similar to those of O_2. Dopamine β-monooxygenase has been shown to be competitively inhibited by CO with respect to O_2 (*44*); further, CO was concluded to bind specifically at the Cu_B center (*45*). Boswell et al. (*46*) extended the study of the binding of CO to reduced PAM and found the stoichiometry of CO binding to be identical to that of DβM, 0.5 CO per Cu(I). Characterization of the PAM·CO complex by FTIR further supported the similarity between the carbonyl complexes formed with DβM and PAM. One difference between DβM and PAM is that DβM shows a random steady-state mechanism in the absence of fumarate (see below) such that kinetic data support a productive binding of O_2 (CO) to enzyme in the absence of substrate. In the case of PAM, the formation of a productive CO complex in the absence of peptide substrate would not be predicted from the kinetic mechanism described herein. It could be argued that O_2 binding to PAM can occur in a catalytically competent mode but that the rate of substrate binding always exceeds that of O_2 binding under turnover conditions.

Table 4: Microscopic Rate Constants for PHM According to Scheme 3[a]

k_3 (mM^{-1} s^{-1})	227 ± 7
k_4 (s^{-1})	185 ± 28
k_5 (s^{-1})	810 ± 120
k_7 (s^{-1})	41 ± 1

[a] Calculated from the equations derived in ref *47* (eq 1−8, Table 6), as they apply to an equilibrium ordered mechanism. The kinetic parameters that lead to k_3, k_4, k_5, and k_7 were obtained with protio vs dideuterio hippuric acids so that the intrinsic isotope effect used in these calculations (12.7 ± 1.0) is the product of the intrinsic primary and α-secondary isotope effects. The value of $^{\alpha-D}k$ was obtained from an $^{\alpha-T}k$ measurement with protium in the primary (cleaved) position. In the instance of tunneling and coupled motion (cf. ref *57* and the text), the magnitude of $^{\alpha-D}k$ may be reduced with deuterium in the primary position. Using an $^{\alpha-D}k$ of 1.10, for example, to calculate rate constants, we obtain final values that are within experimental error of those listed above.

When the magnitude of the intrinsic isotope effect ($^Dk_5$) is known, kinetic isotope effects measurements can provide individual rate constants. Ahn and Klinman (*47*) derived equations for the calculation of the microscopic rate constants for a steady-state random mechanism. These equations can also be applied to an equilibrium ordered mechanism (Scheme 3). This technique requires a $^DV_{max}$ parameter isotope effect different from unity and, thus, in this study has only been useful for PHM. Calculated rate constants and their corresponding errors for PHM are summarized in Table 4.

Ahn and Klinman (*47*) were able to determine the microscopic rate constants for DβM as a function of pH and the activator fumarate. Data for DβM at pH 6.0 indicated a change in kinetic order depending on whether the anionic activator fumaric acid was present. With fumarate in the assay buffer, dopamine is the "stickier" substrate, dissociating approximately 11-fold slower than oxygen from the ternary complex; however, in the absence of fumarate, oxygen dissociates approximately 2-fold faster than dopamine. In other words, the steady-state random kinetic mechanism for DβM at pH 6.0 in the presence of fumarate becomes steady-state ordered, with dopamine binding first followed by O_2. As noted above, in the case of glycine extended peptides with additional binding interactions, the kinetic mechanism for PHM may become steady-state ordered instead of the equilibrium ordered mechanism seen with hippuric acid. It may be significant that the net charge for bound dopamine plus fumarate (−1) is the same as that for preferred peptide substrates (−1) of PAM and PHM.

A comparison of isotope effects for PAM and PHM provides possible insight into functional differences between these two monooxygenating forms. While the isotope effects on V/K for both hippuric acid and oxygen are similar, the isotope effect on V_{max} is different. In the case of PHM, $^DV_{max}$ equals 1.56 ± 0.07; for PAM, there is no isotope effect, with $^DV_{max}$ equal to 1.00 ± 0.08. The smaller $^DV_{max}$ isotope effect with the bifunctional PAM implicates a release of product slower and more rate-determining than that for the monofunctional enzyme PHM. This is an intriguing result, suggesting a possible channeling of the hydroxylated peptide product from the monooxygenase to the lyase domain within the bifunctional PAM.

Comparison of Intrinsic Parameters to Those of DβM. For systems in which the C−H bond cleavage is essentially

irreversible, Northrop's method for determining the intrinsic isotope effects provides a single solution (*36*). The irreversibility of the C−H bond cleavage for peptidyl α-amidating enzyme has not been determined, as was done for dopamine *β*-monooxygenase (*37*); however, we consider this an excellent assumption. In this study, the intrinsic isotope effect for the C−H bond cleavage catalyzed by PHM was determined using hippuric acid as a substrate. A competitive method using remote radiolabeled substrates yields very accurate measurements of the isotope effects on V/K_{HA}, in most cases, with errors of <3%. The primary deuterium intrinsic isotope effect for PHM is thus 10.6 ± 0.8, and the α-secondary deuterium intrinsic isotope effect is 1.20 ± 0.03 (Table 3). The intrinsic isotope effects for the C−H bond cleavage were determined previously for dopamine *β*-monooxygenase with dopamine as a substrate using a similar methodology (*37*, *39*). The magnitudes for the primary and secondary deuterium intrinsic isotope effects for D*β*M are 10.9 ± 1.9 and 1.19 ± 0.06, respectively (Table 3). The similarity between the intrinsic isotope effects for both enzyme systems is remarkable, implying essentially identical transition-state structures. This is, perhaps, not surprising in the context of the magnitude of rate constants and bond dissociation energies in the two systems. The rate constant for the C−H bond cleavage step for PHM with hippuric acid is 810 ± 120 s^{-1} compared to a value of 1200 ± 540 s^{-1} calculated for D*β*M with dopamine as the substrate. The bond dissociation energy for the benzylic C−H bond in dopamine is 85 kcal/mol (*48*) in comparison to a bond dissociation energy of 87 kcal/mol for the C−H of $NH_2CH_2COO^-$ (*49*). It appears that the identical values calculated for the intrinsic isotope effects with PHM and D*β*M reflect similar energetics and, hence, transition-state structures with these two substrates, extending the similarities between these two enzymes significantly beyond sequence homology and cofactor requirements.

From semiclassical considerations, the magnitude of the observed α-secondary intrinsic isotope effects (Table 3) predicts a very product-like transition state, in contrast to the large primary intrinsic isotope effect, which indicates a more symmetrical transition state (*50*). Inflated kinetic α-secondary isotope effects have been observed in a number of dehydrogenase reactions where an sp^3 hybridized methylene carbon center is undergoing conversion to an sp^2 hybridized center (*51*, *52*). This has been attributed to coupled motions between the primary and secondary hydrogens at the transition state (*52*, *53*). Since coupled motions lead to an increase in the secondary isotope effect at the expense of a decrease in the primary isotope effect, the incorporation of a tunneling correction was necessary to model the measured primary isotope effects as well (*54*).

We now suggest that the lack of correspondence between the measured primary and secondary isotope effects, as well as their large magnitudes, may indicate a contribution of nonclassical behavior to both the D*β*M and PHM reactions. In recent years, the degree of tunneling contribution to C−H activation processes in enzyme reactions has been shown to vary from moderate to extreme (*55*). Experimental methods for the detection of tunneling include a demonstration of anomalous temperature dependencies for isotope effects and the breakdown of the semiclassical mass relationship (*56*) between H/T and D/T isotope effects (*57*). Importantly for this study, Grant and Klinman (*58*) have shown that quantum contributions to H transfer can significantly affect the relationship between measured H/T and D/T isotope effects with relatively little impact on the H/T and H/D comparison. Furthermore, since deviations from the Swain−Schaad relationship appear almost exclusively in secondary isotope effect measurements (*59*), they are not expected to affect the calculation of intrinsic isotope effects using eq 5. For the future, it will be very important to confirm and quantitate any tunneling contribution to the PHM and D*β*M reactions. In light of our established protocol for the accurate determination of intrinsic isotope effects with PHM at 37 °C, it may be possible to measure the temperature dependence of $^Dk_5$ (both primary and secondary) directly as a probe of the tunneling behavior in this system.

ACKNOWLEDGMENT

We are grateful to Frank Rhames for the purification of the PHM catalytic core.

REFERENCES

1. Eipper, B. A., Stoffers, D. A., and Mains, R. E. (1992) *Annu. Rev. Neurosci. 15*, 57−85.
2. Merkler, D. J., Kulathila, R., Young, S. D., Freeman, J., and Villafranca, J. J. (1993) in *Bioinorganic Chemistry of Copper* (Karlin, K. D., and Tyeklár, Z., Eds.) pp 196−209, Chapman & Hall, Inc., New York.
3. Merkler, D. J. (1994) *Enzyme Microb. Technol. 16*, 450−456.
4. McMahon, A., Geertman, R., and Sabban, E. L. (1990) *J. Neurosci. Res. 25*, 395−404.
5. Stoffers, D. A., Green, C. B.-R., and Eipper, B. A. (1989) *Proc. Natl. Acad. Sci. U.S.A. 86*, 735−739.
6. Ash, D. E., Papadopoulos, N. J., Colombo, G., and Villafranca, J. J. (1984) *J. Biol. Chem. 259*, 3395−3398.
7. Klinman, J. P., Krueger, M., Brenner, M., and Edmonson, D. E. (1984) *J. Biol. Chem. 259*, 3399−3402.
8. Kulathila, R., Consalvo, A. P., Fitzpatrick, P. F., Freeman, J. C., Snyder, L. M., Villafranca, J. J., and Merkler, D. J. (1994) *Arch. Biochem. Biophys. 311*, 191−195.
9. Stewart, L. C., and Klinman, J. P. (1987) *Biochemistry 26*, 5302−5309.
10. Brenner, M. C., Murray, C. J., and Klinman, J. P. (1989) *Biochemistry 28*, 4656−4664.
11. Brenner, M. C., and Klinman, J. P. (1989) *Biochemistry 28*, 4664−4670.
12. Freeman, J. C., Villafranca, J. J., and Merkler, D. J. (1993) *J. Am. Chem. Soc. 115*, 4923−4924.
13. Prigge, S. T., Kolhekar, A. S., Eipper, B. A., Mains, R. E., and Amzel, L. M. (1997) *Science 278*, 1300−1305.
14. Kizer, J. S., Bateman, R. C., Jr., Miller, C. R., Humm, J., Busby, W. H., Jr., and Youngblood, W. W. (1986) *Endocrinology 118*, 2262−2267.
15. Murthy, A. S. N., Mains, R. E., and Eipper, B. A. (1986) *J. Biol. Chem. 261*, 1815−1822.
16. Gilligan, J. P., Lovato, S. J., Mehta, N. M., Bertelsen, A. H., Jeng, A. Y., and Tamburini, P. P. (1989) *Endocrinology 124*, 2729−2736.
17. Merkler, D. J., Kulathila, R., Consalvo, A. P., Young, S. D., and Ash, D. E. (1992) *Biochemistry 31*, 7282−7288.
18. Goldstein, M., Joh, T. H., and Garvey, T. Q., III (1968) *Biochemistry 7*, 2724−2730.
19. Fitzpatrick, P. F., Harpel, M. R., and Villafranca, J. J. (1986) *Arch. Biochem. Biophys. 249*, 70−75.
20. Klinman, J. P., Humphries, H., and Voet, J. G. (1980) *J. Biol. Chem. 255*, 11648−11651.
21. Cook, P. F., and Cleland, W. W. (1981) *Biochemistry 20*, 1790−1796.
22. Katopodis, A. G., and May, S. W. (1990) *Biochemistry 29*, 4541−4548.

23. Chen, F. M. F., and Benoiton, N. L. (1987) *Can. J. Chem. 65*, 1224−1227.
24. Anantharamaiah, G. M., and Sivanandaiah, K. M. (1977) *J. Chem. Soc., Perkin Trans. 1*, 490−491.
25. Gani, O., Wallis, C., and Young, D. W. (1983) *Eur. J. Biochem. 136*, 303−311.
26. Lockley, W. J. S. (1985) *J. Chem. Res., Synop.*, 178−179.
27. Venkataraman, K., and Wagle, D. R. (1979) *Tetrahedron Lett.*, 3037−3040.
28. Denu, J. M., and Fitzpatrick, P. F. (1994) *Biochemistry 33*, 4001−4007.
29. Matthews, D. E., Piparo, K. E., Burkett, V. H., and Pray, C. C. (1994) in *Animal Cell Technology: Products of Today, Prospects for Tomorrow* (Spier, R. E., Griffiths, J. B., and Berthold, E., Eds.) pp 315−319, Butterworth-Heinemann Ltd., Oxford, U.K.
30. Miller, D. A., Sayad, K. U., Kulathila, R., Beaudry, G. A., Merkler, D. J., and Bertelsen, A. H. (1992) *Arch. Biochem. Biophys. 298*, 380−388.
31. Kolhekar, A. S., Keutmann, H. T., Mains, R. E., Quon, A. S. W., and Eipper, B. A. (1997) *Biochemistry 36*, 10901−10909.
32. Cleland, W. W. (1979) *Methods Enzymol. 63*, 103−138.
33. Bundgaard, H., and Kahns, A. H. (1991) *Peptides 12*, 745−748.
34. Mournier, C. E., Shi, J., Sirimanne, S. R., Chen, B.-H., Moore, A. B., Gill-Woznichak, M. M., Pind, D., and May, S. W. (1997) *J. Biol. Chem. 272*, 5016−5023.
35. Rudolph, F. B., and Fromm, H. J. (1979) *Methods Enzymol. 63*, 138−158.
36. Northrop, D. B. (1975) *Biochemistry 14*, 2644−2651.
37. Miller, S. M., and Klinman, J. P. (1983) *Biochemistry 22*, 3091−3096.
38. Northrop, D. B. (1991) in *Enzyme Mechanism from Isotope Effects* (Cook, P. F., Ed.) pp 181−202, CRC Press, Boca Raton, FL.
39. Miller, S. M., and Klinman, J. P. (1985) *Biochemistry 24*, 2114−2127.
40. Tamburini, P. P., Jones, B. N., Consalvo, A. P., Young, S. D., Lovato, S. J., Gilligan, J. P., Wennogle, L. P., Erion, M., and Jeng, A. Y. (1988) *Arch. Biochem. Biophys. 267*, 623−631.
41. Tamburini, P. P., Young, S. D., Jones, B. N., Palmesino, R. A., and Consalvo, A. P. (1990) *Int. J. Pept. Protein Res. 35*, 153−156.
42. Li, C., Oldman, C. D., and May, S. W. (1994) *Biochem. J. 300*, 31−36.
43. LaReau, R. D., Wan, W., and Anderson, V. E. (1989) *Biochemistry 28*, 3619−3624.
44. Blackburn, N. J., Pettingill, T. M., Seagraves, K. S., and Shigeta, R. T. (1990) *J. Biol. Chem. 265*, 15383−15386.
45. Reedy, B. J., and Blackburn, N. J. (1994) *J. Am. Chem. Soc. 116*, 1924−1931.
46. Boswell, J. S., Reedy, B. J., Kulathila, R., Merkler, D., and Blackburn, N. J. (1996) *Biochemistry 35*, 12241−12250.
47. Ahn, N., and Klinman, J. P. (1983) *Biochemistry 22*, 3096−3106.
48. Weast, R. C., Ed. (1971) *CRC Handbook of Chemistry and Physics*, 51st ed., The Chemical Rubber Co., Cleveland, OH.
49. Armstrong, D. A., Yu, D., and Rauk, A. (1996) *Can. J. Chem. 74*, 1192−1199.
50. Gandour, R. D., and Schowen, R. L. (1978) *Transition States of Biochemical Processes*, Plenum Press, New York.
51. Welsh, K. M., Creighton, D. J., and Klinman, J. P. (1980) *Biochemistry 19*, 2005−2016.
52. Cook, P. F., Oppenheimer, N. J., and Cleland, W. W. (1981) *Biochemistry 20*, 1817−1825.
53. Kurz, L. C., and Frieden, C. (1980) *J. Am. Chem. Soc. 102*, 4198−4203.
54. Huskey, W. P., and Schowen, R. L. (1983) *J. Am. Chem. Soc. 105*, 5704−5706.
55. Kohen, A., and Klinman, J. P. (1998) *Acc. Chem. Res.* (in press).
56. Swain, C. G., Stivers, E. C., Reuwer, J. F., Jr., and Schaad, L. J. (1958) *J. Am. Chem. Soc. 80*, 5885−5893.
57. Bahnson, B. J., and Klinman, J. P. (1995) *Methods Enzymol. 249*, 373−397.
58. Grant, K. L., and Klinman, J. P. (1992) *Bioorg. Chem. 20*, 1−7.
59. Rucker, J. B. (1995) Ph.D. Thesis, University of California, Berkeley, CA.

BI973004Y